Inorg. Chem. **2008**, *47*, 1765−1778

Forum

In Search of Elusive High-Valent Manganese Species That Evaluate Mechanisms of Photosynthetic Water Oxidation

Vincent L. Pecoraro* and Wen-Yuan Hsieh

Departments of Chemistry and Biophysics, The University of Michigan, Ann Arbor, Michigan 48109-1055

Received September 5, 2007

Significant progress in the understanding of biological water oxidation has occurred during the past 25 years. Today we have a somewhat clearer description of the structure of the Mn_4Ca cluster and an idea of the appropriate oxidation states for the enzyme during catalysis. At issue is the mechanism of water oxidation. Depending on one's belief of the manganese ion oxidation levels at the catalytically active S_4 configuration, one can invoke a variety of different processes that could lead to water oxidation. We have suggested that the most likely process is the nucleophilic attack of a water bound to calcium (or manganese) onto a highly electrophilic Mn^{V}═O center. In this Article, we explore the difficulties of preparing Mn^{V} in dimeric systems and the even more arduous task of definitively assigning oxidation states to such highly reactive species.

Introduction

On paper, water oxidation really is a rather simple reaction. Take two molecules of water, oxidize them, and release four protons, as depicted in eq 1.

$$2H_2O \rightarrow O_2 + 4H^+ + 4e^- \quad (0.89\ V/e^-\ \text{at pH 6}) \qquad (1)$$

$$4H^+ + 4e^- \rightarrow 2H_2 \qquad (2)$$

$$2H_2 + O_2 \rightarrow 2H_2O \qquad (3)$$

Water oxidation is the engine that drives higher plant and algal photosynthesis, which ultimately captures nearly all biological energy on earth.[1] Water oxidation also promises to be essential to any futuristic hydrogen economy because from both resource and ecological perspectives the ideal cycle for generating and burning dihydrogen should invoke a step where water is oxidized to dioxygen (a combination of eqs 1 and 2) and dioxygen is converted to water (eq 3). Amazingly, despite its importance to bioenergetics and geopolitical/economic stability, the mechanism of water oxidation and functional models are, at best, poorly described. This *Inorganic Chemistry* Forum focuses on several aspects of this amazing process ranging from understanding fully the structure and function of the oxygen-evolving complex (OEC) of photosystem II (PS II) to chemical water oxidation systems requiring ruthenium. Our specific contribution to this collection of articles is to address the role of small-molecule bioinorganic models for defining the mechanism of photosynthetic water oxidation. The interested reader is referred to reviews for other discussions of small-molecule manganese complexes and their role in understanding photosynthesis.[1–3]

Bioenergetics of Water Oxidation

While described more fully in other articles in this Forum, it is worth spending a short time examining the structural and enzymological features of PS II, the workhorse of higher plant photosynthesis.[1] PS II is embedded within the thylakoid membrane of the chloroplast. Originally, it was thought that

* To whom correspondence should be addressed. E-mail: vlpec@umich.edu.

(1) (a) Wydrzynski, T. *Photosystem II: The Light-Driven Water: Plastoquinone Oxidoreductase*; Springer: New York, 2005. (b) Tommos, C.; Babcock, G. T. *Acc. Chem. Res.* **1998**, *31*, 18–25. (c) McEvoy, J. P.; Brudvig, G. W. *Chem. Rev.* **2006**, *106*, 4455–4483. (d) Yocum, C. F.; Pecoraro, V. L. *Curr. Opin. Chem. Biol.* **1999**, *3*, 182–187. (e) Yachandra, V. K.; Sauer, K.; Klein, M. P. *Chem. Rev.* **1996**, *96*, 2927.

(2) (a) Lewis, N. S.; Nocera, D. G. *Proc. Natl. Acad. Sci. U.S.A.* **2006**, *103*, 15729. (b) Crabtree, G. W.; Lewis, N. S. *Phys. Today* **2007**, *60*, 37. (c) Nocera, D. G. *Daedalus* **2006**, *135*, 112.

(3) (a) Wieghardt, K. *Angew. Chem.* **1989**, *101*, 1179. (b) Law, N. A.; Caudle, M. T.; Pecoraro, V. L. *Adv. Inorg. Chem.* **1999**, *46*, 305. (c) Pecoraro, V. L.; Baldwin, M. J.; Gelasco, A. *Chem. Rev.* **1994**, *94*, 807. (d) Mukhopadhyay, S.; Mandal, S. K.; Bhaduri, S.; Armstrong, W. H. *Chem. Rev.* **2004**, *104*, 3981. (e) Wu, A. J.; Penner-Hahn, J. E.; Pecoraro, V. L. *Chem. Rev.* **2004**, *104*, 903. (f) Pecoraro, V. L. *Photochem. Photobiol.* **1988**, *48*, 249.

10.1021/ic7017488 CCC: $40.75
Published on Web 03/10/2008

the reaction center, P_{680}, captured a photon of visible light ($\lambda = 680$ nm) and was promoted to a virtual state that served as a reductant of photopigments such as chlorophyll, pheophytin, and quinones. Workers in the ultrafast community[4] have now shown that energy transfer occurs at the site of chlorophyll a (Chlor) and pheophytin D_1 ($PheoD_1$), generating an initial $Chlor^+PheoD_1^-$ state, with the electron transferring to the quinone and chlorophyll reduction achieved by P_{680}. P_{680}^+ directly serves to oxidize a protein-bound tyrosine, Y_z, which serves as an electron-transfer conduit to the water oxidation center (a cluster of four manganese, one calcium, and possibly chloride and carbonate) known as the oxygen-evolving complex (OEC). A 680 nm photon contains 1.8 eV. This energy must be apportioned between the reductive reactions necessary for plant growth and the oxidative reactions that generate protons used for making adenosine triphosphate. It is thought that approximately 0.6−0.7 V is necessary for driving the reactions of the "reducing side" of the enzyme (ultimately generating a doubly reduced quinone known as Q_B that transfers the newly generated electrons from PS II to membrane acceptor proteins that shuttle these reducing equivalents to photosystem I). Because 0.6 V is used on the reducing side of the reaction, the oxidizing side of the process is left with 1.2 eV to oxidize water. Recent direct determinations of the P_{680}^+/P_{680} potential have given 1.25[5a] and 1.26 V.[5b] At first blush, this should not be a problem because, at the slightly acidic pH conditions of the thylakoid, only 0.89 V/e^- is required for this process. However, one must recognize that photosynthesis must be a high-quantum-yield reaction and requires at least one intermediate oxidant, Y_z^+. Therefore, some of this excess energy must be lost to attain a near-unity quantum yield. It has been estimated that 100 mV is necessary to drive each oxidation step (P_{680}^+/Y_z to P_{680}/Y_z^+ and Y_z^+/OEC^n to Y_z/OEC^{n+1}). Lavergne and Diner[5b] have estimated the S_2/S_1 potential to be 1.02 V. Obviously, this means there is only ~1.0 V of useful oxidizing power to drive the reaction.

In the early 1980s, many workers struggled to understand how such a strongly oxidized cofactor could be found in biology.[3f] It was well-known by the late 1960s and early 1970s, based on the pioneering work of Pierre Joliot[6a–c] and Bessel Kok[6d] that had placed the kinetic mechanism of water oxidation in clear view, that four oxidizing equivalents were required for water oxidation. Kok described this via the *S* cycle shown in Figure 1 (this version of the *S* clock shows an S_4* state that was uncovered very recently[6e]). This series

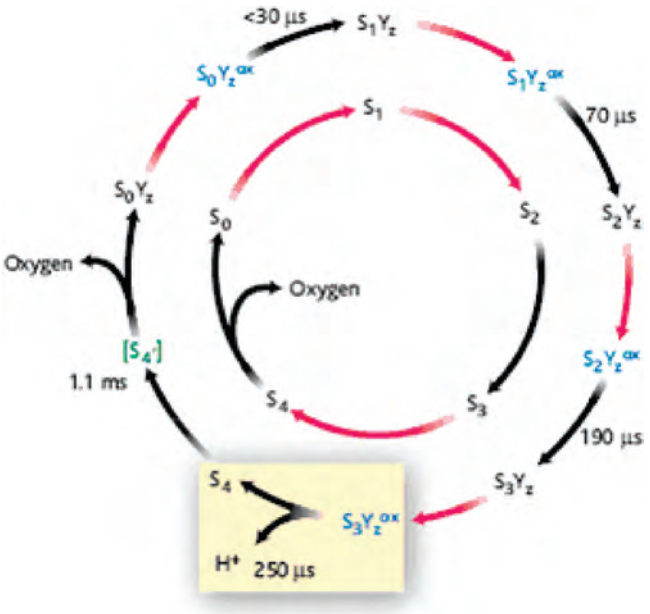

Figure 1. Diagram of the *S* clock, which describes the five intermediate oxidation states of the OEC. S_0 is the product state after dioxygen has been released, S_1 is the stable oxidation level in the dark, and the transition $S_3 \rightarrow S_4 \rightarrow S_0$ is the step leading to dioxygen production and release. The S_4* state has recently been reported. Reproduced with permission from ref 6.

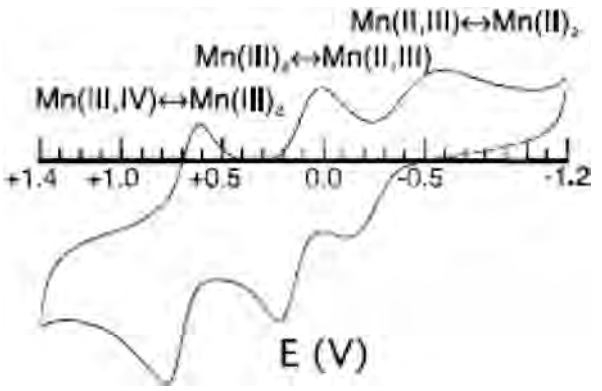

Figure 2. Cyclic voltammogram for the successive oxidation of [Mn(2-OHSalpn)]$_2$ complexes illustrating the large energy separation between each successive dimer oxidation. Reproduced from ref 7.

of photochemically driven reactions invokes five OEC redox intermediates known as states and abbreviated as S_0-S_4. The most reduced state is S_0, the most oxidized state is S_4, and the transition from $S_3 \rightarrow S_4 \rightarrow S_0$ corresponds to the critical step where dioxygen is formed and released. As discussed above, the amount of energy available to oxidize each of these states is a uniform 1.0 V. With the information provided, there appeared to be no problem with these energetics; however, we pointed out in the early 1990s that there was an even more vexing problem that biology needed to overcome. That problem was the accumulation of four oxidizing equivalents on a manganese oxo cluster *maintained within the proper potential range* and unable to participate in unwanted side reactions. As was illustrated by the successive oxidations of a manganese compound [Mn(2-OHSalpn)]$_2$, which we described some years ago[7] (but which had been known for other small metal aggregates for many years before this), each successive oxidation of a metal ion

(4) (a) Groot, M. L.; Pawlowicz, N. P.; Van Wilderen, L. J. G. W.; Breton, J.; van Stokkum, I. H. M.; van Grondelle, R. *Proc. Natl. Acad. Sci. U.S.A.* **2005**, *102*, 13087. (b) Ishikita, H.; Biesiadka, J.; Loll, B.; Saenger, W.; Knapp, E.-W. *Angew. Chem., Int. Ed.* **2006**, *45*, 1964.
(5) (a) Grabolle, M.; Dau, H. *Biochim. Biophys. Acta, Bioenerg.* **2005**, *1708*, 209. (b) Rappaport, F.; Guergova-Kuras, M.; Nixon, P. J.; Diner, B. A.; Lavergne, J. *Biochemistry* **2002**, *41*, 8518.
(6) (a) Joliot, P. *Brookhaven Symp. Biol.* **1966**, 418. (b) Joliot, P. *Biochim. Biophys. Acta* **1965**, *102*, 116. (c) Joliot, P.; Joliot, A. *Biochim. Biophys. Acta* **1973**, *305*, 302. (d) Kok, B.; Forbush, B.; McGloid, M. *Photochem. Photobiol.* **1970**, *11*, 457. (e) Haumann, M.; Liebisch, P.; Muller, C.; Barra, M.; Grabolle, M.; Dau, H. *Science* **2005**, *310*, 1019.
(7) (a) Gelasco, A.; Kirk, M. L.; Kampf, J. W.; Pecoraro, V. L. *Inorg. Chem.* **1997**, *36*, 1829. (b) Gelasco, A.; Pecoraro, V. L. *Inorg. Chem.* **1998**, *37*, 3301.

in a cluster causes the subsequent oxidation of the cluster to occur at higher potential (between 250 and 500 mV higher) unless there is a concomitant loss of the newly accumulated positive charge. Notice that this concept is different from examination of a Pourbaix diagram, in which one evaluates the pH dependence of a single redox couple as a function of the pH. In this case, we are comparing different redox couples restricted to the same pH conditions. One might also argue that a significant structural change of a cluster could mitigate this principle; however, we would contend that this significantly structurally changed cluster is really a new molecule in its own right. For example, the [Mn(2-OHSalpn)]$_2$ system has approximately 300 mV shifts in potential each time the manganese ions are oxidized. If the same principle is applied to the OEC, oxidation of the manganese ions would engender an approximately 300 mV shift in potential. Recognizing that the maximum potential for any S transition can only be ~1 V, this would require that the less oxidizing transitions be at 0.7 V ($S_2 \rightarrow S_3$), 0.4 V ($S_1 \rightarrow S_2$), and 0.1 V ($S_0 \rightarrow S_1$). The sum of these potentials is 2.2 V, far from the 0.89 V/e$^-$ (~3.6 V) necessary for water oxidation. This discussion has not yet considered the second significant problem with the potential range.

PS II is formed from subunits that appeared by gene duplication, suggesting that the redox-active tyrosine Y_z might have a symmetry-related and redox-active tyrosine in the second subunit. This, in fact, is the case, with the second tyrosine being given the designation tyrosine-D or Y_D.[8] In the old photosynthetic literature, Y_z and Y_D are referred to as signal 2_{fast} and signal 2_{slow}, respectively, based on their electron paramagnetic resonance (EPR) relaxation behavior. We now know that the lifetimes are a consequence of the distance of the tyrosines from the paramagnetic manganese cluster in the OEC. In addition, it appears that while Y_z has a potential of around 1 V, the oxidation potential of Y_D may be significantly less than this (as low as 0.76 V).[9] It has long been known that PS II preparations that are kept in the dark overnight will convert from S_0 to S_1, with the subsequent reduction of Y_D^+ to Y_D.[10] Why this manganese oxidation occurs and whether it is critical to the normal water oxidation process have been subjects of keen speculation (e.g., Y_D^+ may protect the fragile S_0 manganese cluster from destruction by oxidizing it to the less labile S_1 form). For us, however, the *raison d'etre* of the process is unimportant, but simply that it occurs is critical. This is because the S_0 to S_1 oxidation by Y_D^+ provides a lower limit for the manganese oxidation potential in S_0. This value then is ~0.6 V. Therefore, if 3.6 V of the oxidizing power is required to oxidize water, if the first step only provides 0.6 V to this sum, and if the maximal potential on any transition is at most ~1 V, then the remaining transitions must be accumulating the maximum available potential at each step. Now, of course, there is some slop in these numbers. Possibly, S_0-S_1 occurs at 0.7 V, and possibly each oxidation has a maximal 1.1 V potential. Nonetheless, the concerns raised by this analysis are troubling.

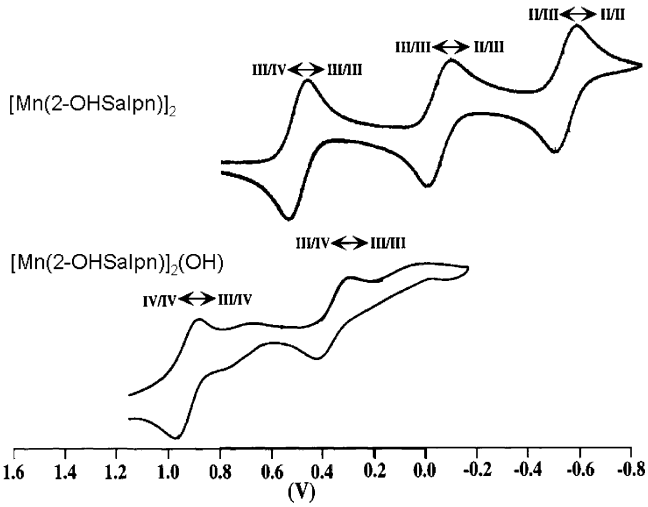

Figure 3. Comparison of cyclic voltammograms for {[Mn^{III}(2-OHSalpn)]$_2$H$_2$O} and {$Mn^{III}Mn^{IV}$(2-OHSalpn)$_2$OH} illustrating how the potential for a Mn^{III}_2 to Mn^{III}/Mn^{IV} transition is nearly at the same potential as a Mn^{III}/Mn^{IV} to Mn^{IV}_2 oxidation when a proton has been removed from a bound ligand. Adapted from ref 13.

The only way to avert the energetic penalty associated with cluster oxidation is to have a charge-invariant transition or to have a major cluster structural change (presumably in a process in which the addition of a ligand cancels the added positive charge). The simplest way to achieve a charge-invariant cluster is to lose a proton (alternatives would include the addition of an anionic ligand such as chloride[11] or (bi)carbonate[12]). This principle is illustrated in Figure 3 using the related complex {[Mn(2-OHSalpn)]$_2$H$_2$O},[13] which has a bound water molecule that can be deprotonated to form a hydroxide complex. Thus, the potential of {[Mn^{III}(2-OHSalpn)]$_2$H$_2$O} is within 50–100 mV of the more highly oxidized {$Mn^{III}Mn^{IV}$(2-OHSalpn)$_2$OH}. The studies of proton release in PS II are too numerous to recount here, but it is well accepted that on at least several steps a proton departs the vicinity of the manganese cluster upon an S transition.[14] Thus, we can conclude that the energetic constraints of the system require proton loss, anion complexation, or cluster structure rearrangement during the steps preceding water oxidation and release. Interestingly, all three of these possibilities have been suggested at some point in the photosynthetic literature (although not always with the recognition that such processes may be essential for the enzyme to progress through its redox cycle).

(8) Faller, P.; Debus, R. J.; Brettel, K.; Sugiura, M.; Rutherford, A. W.; Boussac, A. *Proc. Natl. Acad. Sci. U.S.A.* **2001**, *98*, 14368.
(9) (a) Boussac, A.; Etienne, A. L. *Biochim. Biophys. Acta* **1984**, *766*, 576. (b) Vass, I.; Styring, S. *Biochemistry* **1991**, *30*, 830.
(10) Styring, S.; Rutherford, A. W. *Biochemistry* **1987**, *26*, 2401.
(11) Wincencjusz, H.; vanGorkom, H. J.; Yocum, C. F. *Biochemistry* **1997**, *36*, 3663.
(12) (a) Dasguptar, J.; van Willigen, R. T.; Dismukes, G. C. *Phys. Chem. Chem. Phys.* **2004**, *6*, 4793. (b) Kovlov, Y. N.; Zharmukhamedov, S. K.; Dismukes, G. C. *Phys. Chem. Chem. Phys.* **2004**, *6*, 4905.
(13) (a) Caudle, M. T.; Riggs-Gelasco, P.; Gelasco, A. K.; Penner-Hahn, J. E.; Pecoraro, V. L. *Inorg. Chem.* **1996**, *35*, 3577. (b) Randall, D. W.; Gelasco, A.; Caudle, M. T.; Pecoraro, V. L.; Britt, R. D. *J. Am. Chem. Soc.* **1997**, *119*, 4481. (c) Caudle, M. T.; Pecoraro, V. L. *Inorg. Chem.* **2000**, *39*, 5831–5837.
(14) (a) Junge, W.; Haumann, M.; Ahlbrink, R.; Mulkidjanian, A.; Clausen, J. *Philos. Trans. R. Soc. London, Ser. B* **2002**, *357*, 1407. (b) Haumann, M.; Mulkidjanian, A.; Junge, W. *Biochemistry* **1997**, *36*, 9304. (c) Lavergne, J.; Junge, W. *Photosynth. Res.* **1993**, *38*, 279.

With the energetics of photosynthetic water oxidation now in hand, one must consider the two great controversies presently gripping researchers of the OEC: what are the cluster oxidation states and what is the cluster structure? We will first deal with the oxidation states of the manganese clusters in each of the five Kok states. An accurate knowledge of the manganese oxidation levels, especially in the product (S_0) and reactant (S_4) states, is essential for any serious consideration of mechanism. Given the limited scope of this paper, we will not cover in detail the arguments for or against each assignment in detail, rather limiting ourselves to a statement of the controversies and indicating our preferred oxidation state assignment. While it might seem most logical to first consider the lowest oxidation levels for the four manganese ions in the OEC, found in S_0, the product state resulting after the liberation of dioxygen, we will instead first examine the oxidation levels of the dark stable S_1 and singly oxidized S_2 states. The reason for starting in the middle of the cycle is that for many years the S_1 and S_2 states were the most easily accessed and studied oxidation levels of the enzyme. Thus, historically these two states were the first with assigned manganese oxidation levels and have served as the underpinning for the assignment of all other manganese oxidation levels in each of the other enzyme oxidation states.

Oxidation State Assignments of Manganese in Each *S* State

While numerous techniques have been used to determine the manganese oxidation state, the approach that appears to be the most generally reliable has been X-ray absorption spectroscopy (XAS) and, more specifically, X-ray absorption near-edge structure (XANES) spectroscopy. The following comments are specifically intended for K-edge XANES because this technique has been the most exhaustively employed, although in recent years the L-edge technique has also been probed to provide oxidation state information.[15] The XANES spectrum provides two areas of interest known as the pre-edge region and the X-ray edge. The pre-edge region is the part of the spectrum where 1s electrons may be absorbed into higher lying p or d orbitals. Thus, the pre-edge region follows normal selection rules and provides information about the electronic structure of the manganese ions. Typically, for manganese, one sees weak absorption due to the 1s → 3d transitions, which are symmetry-forbidden; however, in certain special cases, such as the presence of an Mn=O, one can see significant intensity due to the addition of p character into the d molecular orbital.[16] Because XANES provides oxidation state information for the average of the manganese ions and because the transitions observed for Mn^{II}, Mn^{III}, and Mn^{IV} are quite weak, the pre-edge region has only been used for oxidation or structural assignment in the extreme cases of multiply bonded metal oxos (or nitridos).

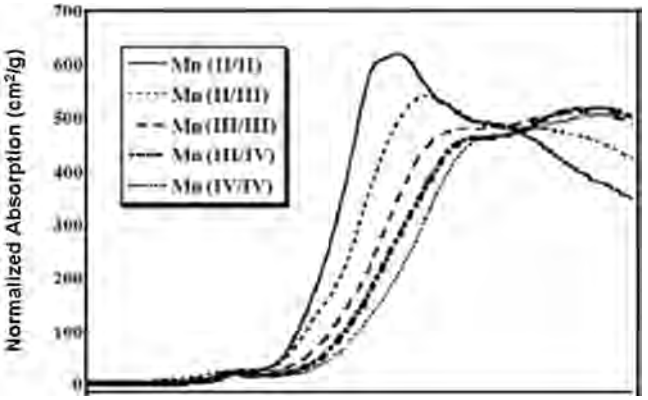

Figure 4. XANES spectra of $[Mn(2\text{-}OHSalpn)]_2$ complexes illustrating how the edge energy increases as the oxidation state of the complex increases. Spectra from left to right correspond to Mn^{II}_2, $Mn^{II}Mn^{III}$, Mn^{III}_2, and $Mn^{III}Mn^{IV}$. Reproduced from ref 7.

In contrast, the X-ray edge, basically corresponding to the photoelectron experiment, looks at the energy required to promote the 1s core–electron into the continuum. A simplified, though not exact, way of understanding the relationship between the oxidation state and edge energy is that the higher the oxidation level of the ion being probed is, the harder it will be to remove this core–electron and the higher will be the energy necessary to remove this 1s electron. This general trend is shown for a series of isostructural $[Mn(2\text{-}OH\ Salpn)]_2^{2-\ to\ 1+}$ complexes in Figure 4.[7] Of course, other factors such as ligand charge, type of bonding, and coordination number complicate this simple picture; however, the general trend with manganese is that the higher oxidation state usually leads to the higher edge energy. However, what might appear to be a more philosophical question (what is the edge energy?) has led to significant disagreement over oxidation state assignment.

Generally speaking, there are three ways in which edge energies have been extracted from the XANES spectrum. The first of these assigns the edge as the first inflection point in the edge spectrum,[17] which can be identified by the first zero crossing in the derivative spectrum. The second approach defines the edge energy as the energy at half-height

(15) (a) Messinger, J.; Robblee, J. H.; Bergmann, U.; Fernandez, C.; Glatzel, P.; Visser, H.; Cinco, R. M.; McFarlane, K. L.; Bellachio, E.; Pizarro, S. A.; Cramer, S. P.; Sauer, K.; Klein, M. P.; Yachandra, V. *J. Am. Chem. Soc.* **2001**, *123*, 7804. (b) Glatzel, P.; Bergmann, U.; Yano, J.; Visser, H.; Robblee, J. H.; Gu, W.; de Groot, M. F.; Christou, G.; Pecoraro, V. L.; Cramer, S. P.; Yachandra, V. K. *J. Am. Chem. Soc.* **2004**, *126*, 9946–9959.

(16) (a) Weng, T. C.; Hsieh, W. Y.; Uffelman, E. S.; Gordon-Wylie, S. W.; Collins, T. J.; Pecoraro, V. L.; Penner-Hahn, J. E. *J. Am. Chem. Soc.* **2004**, *126*, 8070. (b) Yano, J.; Robblee, J.; Pushkar, Y.; Marcus, M. A.; Bendix, J.; Workman, J. M.; Collins, T. J.; Solomon, E. I.; DeBeer George, S.; Yachandra, V. K. *J. Am. Chem. Soc.* **2007**, *129*, 12989. (c) Song, W. J.; Seo, M. S.; DeBeer-George, S.; Ohta, T.; Song, R.; Kang, M.-J.; Tosha, T.; Kitagawa, T.; Solomon, E. I.; Nam, W. *J. Am. Chem. Soc.* **2007**, *129*, 1268.

(17) (a) Kirby, J. A.; Goodin, D. B.; Wyrdzynski, T.; Robertson, A. S.; Klein, M. P. *J. Am. Chem. Soc.* **1981**, *103*, 5537. (b) Roelofs, T. A.; Liang, W. C.; Latimer, M. J.; Cinco, R. M.; Rompel, A.; Andrews, J. C.; Sauer, K.; Yachandra, V. K.; Klein, M. P. *Proc. Nat. Acad. Sci. U.S.A.* **1996**, *93*, 3335. (c) Messinger, J.; Robblee, J. H.; Bergmann, U.; Fernandez, C.; Glatzel, P.; Visser, H.; Cinco, R. M.; McFarlane, K. L.; Bellachio, E.; Pizarro, S. A.; Cramer, S. P.; Sauer, K.; Klein, M. P.; Yachandra, V. *J. Am. Chem. Soc.* **2001**, *123*, 7804. (d) Vissier, H.; Anxolabehere-Mallart, E.; Bergmann, U.; Glatzel, P.; Robblee, J. H.; Cramer, S. P.; Girerd, J.-J.; Sauer, K.; Klein, M. P.; Yachandra, V. K. *J. Am. Chem. Soc.* **2001**, *123*, 7804. (e) Liang, W. C.; Roelofs, T. A.; Cinco, R. M.; Rompel, A.; Latimer, M. J.; Yu, W. O.; Sauer, K.; Klein, M. P.; Yachandra, V. *J. Am. Chem. Soc.* **2000**, *122*, 3399.

of the edge.[18] The third approach extracts the energy by fitting a spline curve through all of the points of the edge.[16,19] Each approach has its strengths and weaknesses, which will not be explored herein. Suffice it to say that each approach will give slightly different edge energies. We mentioned above that the average oxidation state of the manganese cluster can be deduced from the edge energy. To do so requires that a series of well-characterized model compounds of established oxidation state have also been probed by XANES spectroscopy to build a calibration curve. If the structure of the biological center is known, it is best to use models that reflect the first coordination sphere ligands and coordination number of the active site. Separate calibration curves for each of these three different analytical methods have been generated using a wide range of models. Regardless of the determination method of edge energies, all workers in the field have agreed that the best formulation for S_1 is a mixture of Mn^{III} and Mn^{IV}. A similar conclusion can be drawn for the S_2 state, and each analysis agrees that the manganese ions in S_2 are slightly more oxidized (by one electron) than those in S_1. A more precise assignment from XANES alone is difficult; however, when EPR spectroscopy is used in conjunction, a better understanding of oxidation states emerges.

The discovery of the multiline EPR spectrum in S_2 by Dismukes and Siderer[20] was one of the most significant steps in garnering a molecular understanding of the manganese cluster in the OEC. The multiline spectrum, shown as Figure 5, contains at least 19 lines with hyperfine separations consistent with a spin delocalized over a mixture of Mn^{III} and Mn^{IV}. The nuclear spin of ^{55}Mn is $^5/_2$ so one expects six hyperfine lines for a mononuclear manganese ion such as Mn^{II}. More than six hyperfine lines is definitive proof that at least two and, in this case, as many as four manganese ions are associated within the cluster. In addition, the localization of the signal at $g = 2$ (and the variable-temperature dependence of the signal) indicates that the multiline arises from an $S = {}^1/_2$ ground state. Because there are four manganese ions, the only way that one can achieve an $S = {}^1/_2$ ground state is for the cluster to be mixed valent. The multiline spectrum (and models for it) has been probed by numerous workers using techniques ranging from continuous-wave X-band, Q-band, and higher frequencies to ENDOR and ESEEM methods.[22–33] In addition, multiline signals in the presence and absence of Ca^{II}, Sr^{II}, inhibitors

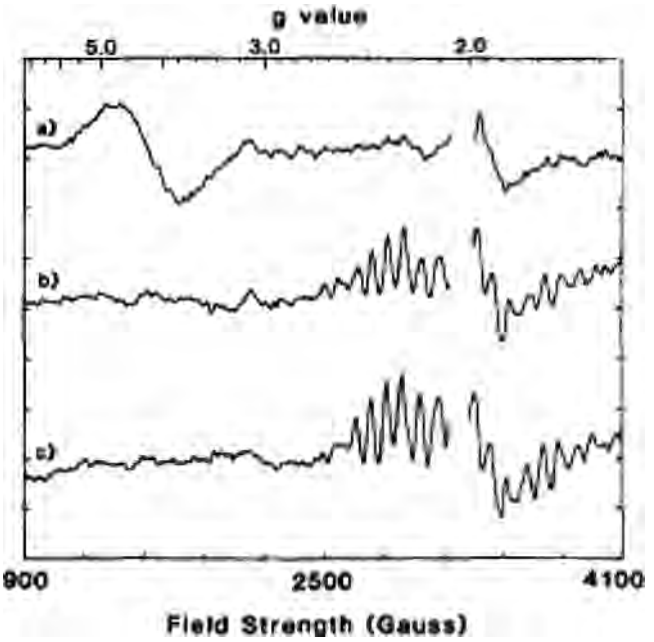

Figure 5. Comparison of a $g = 2$ multiline spectrum of the OEC with that of the "low-field" $g = 4$ signal. The top spectrum is with illumination at 140 K for 30 s, the middle spectrum was warmed to 190 K in the dark for 90 s after illumination at 140 K, and the bottom spectrum is with illumination at 190 K. All spectra were recorded at 10 K. Reproduced with permission from ref 21.

such as ammonia, small molecules such as methanol, and myriad other conditions have been employed to unravel the secrets of this cluster.[34–42]

If we take the XANES observations that S_2 contains only Mn^{III} and Mn^{IV} and is one electron more oxidized that S_1

(18) (a) Ono, T.; Noguchi, T.; Inoue, Y.; Kusunoki, M.; Yamaguchi, H.; Oyangi, H. *J. Am. Chem. Soc.* **1995**, *117*, 6386. (b) Ono, T.; Noguchi, T.; Inoue, Y.; Kusunoki, M.; Yamaguchi, H.; Oyangi, H. *Science* **1992**, *258*, 1335.
(19) (a) Dau, H.; Iuzzolino, L.; Dittmer, J. *Biochim. Biophys. Acta* **2001**, *1503*, 24. (b) Kuntzleman, T.; McCarrick, M.; Penner-Hahn, J.; Yocum, C. *Phys. Chem. Chem. Phys.* **2004**, *6*, 4897. (c) Riggs-Gelasco, P. J.; Mei, R.; Yocum, C. F.; Penner-Hahn, J. E. *J. Am. Chem. Soc.* **1996**, *118*, 2387. (d) Meinke, C.; Sole, V. A.; Pospisil, P. J.; Dau, H. *Biochemistry* **2000**, *39*, 7033.
(20) Dismukes, G. C.; Siderer, Y. *Proc. Natl. Acad. Sci. U.S.A.* **1981**, *78*, 274.
(21) Casey, J. L.; Sauer, K. *Biochim. Biophys. Acta* **1984**, *767*, 21.
(22) Chalot, M. F.; Boussac, A.; Blondin, G. *Biochim. Biophys. Acta* **2005**, *1708*, 120.
(23) (a) Boussac, A. *Biochim. Biophys. Acta* **1996**, *1277*, 253. (b) Boussac, A. *Chem. Phys.* **1995**, *194*, 409.
(24) Teutloff, C.; Kessen, S.; Kern, J.; Zouni, A.; Bittl, R. *FEBS Lett.* **2006**, *580*, 3605.
(25) Zheng, M.; Dismukes, G. C. *Photosynth. Res.* **1992**, *34*, 144.
(26) Miller, A. F.; Brudvig, G. W. *Biochim. Biophys. Acta* **1991**, *1056*, 1.
(27) Beck, W. F.; DePaula, J. C.; Brudvig, G. W. *J. Am. Chem. Soc.* **1986**, *108*, 4018.
(28) DePaula, J. C.; Brudvig, G. W. *J. Am. Chem. Soc.* **1985**, *107*, 2643.
(29) Beck, W. F.; Brudvig, G. W. *Biochemistry* **1986**, *25*, 6479.
(30) Peloquin, J. M.; Campbell, K. A.; Randall, D. W.; Evanchik, M. A.; Pecoraro, V. L.; Armstrong, W. H.; Britt, R. D. *J. Am. Chem. Soc.* **2000**, *122*, 10926.
(31) Peloquin, J. M.; Campbell, K. A.; Britt, R. D. *J. Am. Chem. Soc.* **1998**, *120*, 6840.
(32) Randall, D. W.; Sturgeon, B. E.; Ball, J. A.; Lorigan, G. A.; Chan, M. K.; Klein, M. P.; Armstrong, W. H.; Britt, R. D. *J. Am. Chem. Soc.* **1995**, *117*, 11780.
(33) Britt, R. D.; Peloquin, J. M.; Campbell, K. A. *Annu. Rev. Biophys. Biomol. Struct.* **2000**, *29*, 463.
(34) Britt, R. D.; Zimmermann, J. L.; Sauer, K.; Klein, M. P. *J. Am. Chem. Soc.* **1989**, *111*, 3522.
(35) Kim, D. H.; Britt, R. D.; Klein, M. P.; Sauer, K. *Biochemistry* **1992**, *31*, 541.
(36) Boussac, A.; Rappaport, F.; Carrier, P.; Verbatz, J. M.; Gobin, R.; Kirilovsky, D.; Rutherford, A. W.; Sugiura, M. *J. Biol. Chem.* **2004**, *279*, 22809.
(37) Tyryshkin, A. M.; Watt, R. W. K.; Baranov, S. V.; Dasgupta, J.; Hendrich, M. P.; Dismukes, G. C. *Biochemistry* **2006**, *45*, 12876.
(38) Britt, R. D.; Campbell, K. A.; Peloquin, J. M.; Gilchrist, M. L.; Aznar, C. P.; Dicus, M. M.; Roblee, J.; Messinger, J. *Biochim. Biophys. Acta* **2004**, *1655*, 158.
(39) Sivaria, M.; Tso, J.; DIsmukes, G. C. *Biochemistry* **1989**, *28*, 9459.
(40) Gilchrist, M. L.; Ball, J. A.; Randall, D. W.; Britt, R. D. *Proc. Natl. Acad. Sci. U.S.A.* **1995**, *92*, 9545.
(41) Carrell, T. G.; Tyryshkin, A. M.; Dismukes, G. C. *J. Biol. Inorg. Chem.* **2002**, *7*, 2.
(42) Campbell, K. A.; Peloquin, J. M.; Pham, D. P.; Debus, R. J.; Britt, R. D. *J. Am. Chem. Soc.* **1998**, *120*, 447.

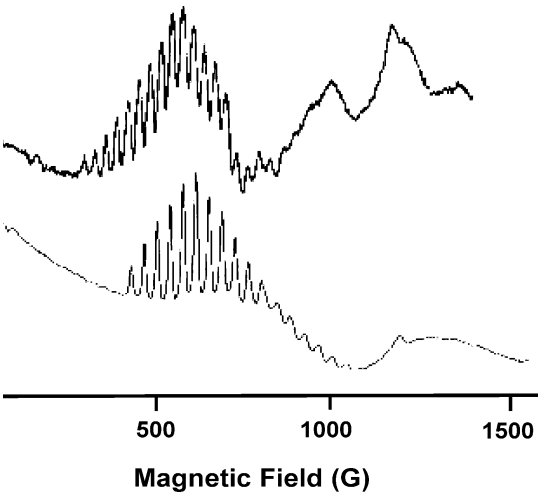

Figure 6. S_1-state parallel-mode EPR spectrum (top). This spectrum is compared to a tetranuclear Mn^{IV}_4 cluster (bottom). Reproduced from ref 43.

and combine this with the EPR observation that S_2 contains an odd number of Mn^{IV} ions (this necessity comes from the fact that Mn^{IV} is a d^3 ion and only an odd number of such ions can yield a nonintegral spin system), then S_2 should be $Mn^{III}Mn^{IV}_3$. A formulation of $Mn^{III}_3Mn^{IV}$ is unlikely because S_1 must contain both Mn^{III} and Mn^{IV}, and we know from the above discussion that the transition from S_1 to S_2 requires a manganese-centered oxidation. Generally speaking, fits to ESEEM, ENDOR, and EPR spectra are consistent with this assignment, although there have been claims that the $Mn^{III}_3Mn^{IV}$ oxidation formulation better fits simulations to the different $g = 2$ multilines formed with the native form and modified multilines.[41]

Given the assignment of S_2 as $Mn^{III}_3Mn^{IV}$, then one-electron reduction of this cluster should yield S_1 as $Mn^{III}_2Mn^{IV}_2$. Such a non-Kramers ion is not expected to show an EPR signal at X-band frequencies using perpendicular-mode detection (the standard cavity alignment); however, it is possible that a parallel-mode-detected experiment can allow for observation of an EPR signal from this integral spin cluster. Figure 6 shows the spectrum that Britt's group isolated for the S_1 state.[42] It too has a multiline structure, but the resonance is centered at lower field. This OEC S_1 signal is compared with the only known spectroscopic model for this S state in Figure 6.[43] The complex $\{[Mn(2\text{-}OHSalpn)]_4O\}^{2+}$ is thought to contain four Mn^{IV} ions. As such, it has a slightly reduced hyperfine coupling compared with the enzymatic signal. This observation is consistent with the S_1 state being slightly reduced compared to the model, which is fully consistent with the assignment of S_1 as $Mn^{III}_2Mn^{IV}_2$.

While the consensus of workers in photosynthesis is in agreement with these oxidation state assignments, the relative unanimity disappears when the remaining S states are discussed. Nowhere is the discussion more vigorous than when considering the transition from S_2 to S_3. One camp basically believes that oxidation of the enzyme occurs on either a ligand or a protein residue, but not at the manganese atoms.[17] The second group is a proponent of manganese-centered oxidation on this transition.[18,19,44–46] The two oxidation formulations can thus be summarized as $Mn^{III}Mn^{IV}_3$(substrate)$^\bullet$ or $Mn^{III}Mn^{IV}_3$(protein)$^\bullet$ for the first model and Mn^{IV}_4 for the second model. The primary basis of this disagreement is associated with the interpretation of the XANES spectra. As discussed above, different groups use different methodologies to define the edge energy. While the differences associated with the different methods are not a significant issue when looking at any one S state, the comparison becomes more difficult when making comparisons between different methods making substractions from adjacent S states. Thus, some workers estimate that the change in edge energy is inconsistent with a manganese-centered oxidation, whereas other workers obtain larger edge-energy differences that are more consistent with manganese-centered oxidation occurring. Compounding these methodological differences is the fact that sample preparation is crucial for obtaining high-quality results and that there is an inherent difficulty in obtaining clean S-state transitions. Early PS II preparations suffered from having either double hits (advancement of the system by two S states with one photon) or misses (despite the addition of a photon, the enzyme is not oxidized).[47] Modern laser methods minimize the number of misses; however, double hits still occur. Thus, depending on the quality of the initial sample, the number of double hits occurring after illumination and the edge analysis all contribute to the various discrepancies. To circumvent these problems, some researchers have gone to L-edge spectra,[17] while others have looked at various types of EPR spectroscopy of S_3 (parallel mode[48] because perpendicular-mode EPR is silent, as might be expected for manganese oxidation). Some models have even suggested the formation of Mn^{IV}=O (oxyl groups) at this oxidation level.[49] We will simply conclude that, in our opinion, the oxidation level of S_3 remains unresolved; however, our reading of the literature gives us the preference for manganese-centered oxidation, yielding Mn^{IV}_4. What can be said definitively about S_3, based on XANES pre-edge spectra, is that this enzyme form does not contain a manganese−oxyl such as Mn^{IV}=O.[16]

Because one cannot define the S_3 state conclusively, it seems a bit premature to provide an assignment for the

(43) Hsieh, W. Y.; Campbell, K. A.; Gregor, W.; Britt, R. D.; Yoder, D. W.; Penner-Hahn, J. E.; Pecoraro, V. L. *Biochim. Biophys. Acta* **2004**, *1655*, 149.

(44) Pecoraro, V. L.; Hsieh, W. Y. In *Metal Ions in Biological Systems*; Sigel, H., Sigel, A., Eds.; Marcel Dekker: New York, 2000; Vol. 37, p 429.

(45) Pecoraro, V. L.; Baldwin, M. J.; Caudle, M. T.; Hsieh, W. Y.; Law, N. A. *Pure Appl. Chem.* **1998**, *70*, 925.

(46) (a) Vrettos, J. S.; Limburg, J.; Brudvig, G. W. *Biochim. Biophys. Acta* **2001**, *1503*, 229. (b) Vrettos, J. S.; Brudvig, G. W. *Philos. Trans. R. Soc. London, Ser. B* **2002**, *357*, 1395. (c) Limburg, J.; Szalai, V. A.; Brudvig, G. W. *J. Chem. Soc., Dalton Trans.* **1999**, 1353.

(47) (a) Shinkarev, V. *Biophys. J.* **2005**, *88*, 412. (b) Jursinic, P. *Biochim. Biophys. Acta* **1981**, *635*, 38.

(48) (a) Ioannidis, N.; Nugent, J. H. A.; Petrouleas, V. *Biochemistry* **2002**, *41*, 9589. (b) Ioannidis, N.; Petrouleas, V. *Biochemistry* **2002**, *41*, 9580. (c) Ioannidis, N.; Zahariou, G.; Petrouleas, V. *Biochemistry* **2006**, *45*, 6252.

(49) (a) Hoganson, C.; Babcock, G. T. *Science* **1997**, *277*, 1953. (b) Tommos, C.; Babcock, G. T. *Acc. Chem. Res.* **1998**, *31*, 18.

catalytically active S_4 level. Nonetheless, if one wants to assess mechanistic options for water oxidation, some working hypothesis for S_4 must be forwarded. The same questions that plagued the $S_2 \rightarrow S_3$ transition again arise: Is the enzyme oxidation centered on manganese or elsewhere and, if elsewhere, is the location a protein residue or the substrate? It is known that oxygen production is concurrent with rereduction of Y_z^+; therefore, it seems highly unlikely that a protein residue (i.e., amino acid) could first be oxidized followed by substrate or metal oxidation and still follow these fast kinetics. If oxidation to form S_3 yields a substrate radical, then formation of S_4 could consist of a biradical substrate species (i.e., two oxygen radicals bound to the cluster). Because we prefer the $Mn^{IV}{}_4$ formalism for S_3, we are left with either a $Mn^{IV}{}_3Mn^{V}$ or a $Mn^{IV}{}_4$(substrate)$^{\bullet}$ species. The ligand usually invoked for the latter possibility is a manganyl−oxo atom[50] or a bridging μ-oxo ligand.[17] There have been no experiments that directly probe these three possibilities; however, computational studies have tended to support the $Mn^{IV}O$(radical) except for recent QM/MM studies.[51] In some senses, the difference may be semantic in that a molecular orbital with significant manganese and oxygen character could be the source of this last electron. However, there is a subtle difference in the reaction pathway that would be predicted between these two formulations. This difference will be discussed in more detail below.

Before leaving manganese oxidation assignments, we must address the product state of the system, S_0. For years, it was tacitly assumed that if S_1 contained $Mn^{III}{}_2Mn^{IV}{}_2$, then the one-electron-reduced enzyme would best be formulated as $Mn^{III}{}_3Mn^{IV}$. Such a system should be EPR-active, and yet it was only within the past decade that a perpendicular-mode X-band spectrum has been reported (and only in the presence of methanol).[52] The $g = 2$ multiline signal for S_0 suggests an $S = {}^1/_2$ ground state, and the spacing of the hyperfine lines is consistent with a lower oxidation level than the S_2 multiline previously reported. Subsequent analysis of the EPR spectrum seemed to indicate that Mn^{II} could be present in S_0. Further XANES data were also consistent with this idea.[17a,53] If Mn^{II} is present in S_0, then one must reevaluate the total manganese oxidation assignment. The simplest possibility is that S_0 could have manganese existing in three different oxidation levels such as $Mn^{II}Mn^{III}Mn^{IV}{}_2$. Such a formulation is not without precedent as Armstrong[54] demonstrated that Mn^{II}, Mn^{III}, and Mn^{IV} could coexist in a single structure. Subsequently, Kessissoglou et al.[55] reported a tetrameric cluster with manganese composition $Mn^{II}{}_3Mn^{IV}$ and we prepared a trinuclear $Mn^{II}Mn^{IV}Mn^{II}$ system.[56] In an effort to assess whether XANES spectroscopy was capable of distinguishing oxidation state formulations for redox isomers, we examined two $Mn_3{}^{8+}$ structures having compositions $Mn^{II}Mn^{IV}Mn^{II}$ and $Mn^{III}Mn^{II}Mn^{III}$ [57] and showed that, at least for trinuclear systems, XANES could distinguish outside of experimental error the proper oxidation assignments for these molecules.[56] A recent study[56c] suggests that this is a more difficult proposition when tetranuclear $Mn_4{}^{10+}$ complexes are studied (i.e., $Mn^{II}{}_2Mn^{III}{}_2$ vs $Mn^{II}{}_3Mn^{IV}$). Not surprisingly, more recent studies have supported the previous $Mn^{III}{}_3Mn^{IV}$.[58] In this case, it may be that both formulations are correct because the answer that one gets may be related to how S_0 is prepared. Thus, for the purposes of this Article, we will assume that either $Mn^{III}{}_3Mn^{IV}$ or $Mn^{II}Mn^{III}Mn^{IV}{}_2$ can exist and that they may even interconvert under appropriate circumstances.

In summary, the oxidation state assignments of the manganese ions in the OEC are still controversial. Consensus supports manganese oxidation from S_0 to S_1 and from S_1 to S_2. There are two schools of thought on enzyme oxidation beyond S_2, with manganese-centered, protein-centered, and ligand-centered oxidation all proposed. The S_1 level is almost certainly a mixture of Mn^{III} and Mn^{IV}, with $Mn^{III}{}_2Mn^{IV}{}_2$ most likely. Formation of S_2 probably yields $Mn^{III}Mn^{IV}{}_3$. Our preference that this is to form a $Mn^{IV}{}_3Mn^{V}$ species in S_4, although computational studies support an $Mn^{IV}{}_4$(substrate)$^{\bullet}$. After dioxygen is released, S_0 may contain either $Mn^{II}Mn^{II}{}_{1}Mn^{IV}{}_2$ or $Mn^{III}{}_3Mn^{IV}$. With this understanding of the single ion structure of the manganese atoms, we will now consider the structure of the $CaMn_4$ cluster.

Structure of the Mn_4Ca Cluster

While there is an extremely rich and interesting scientific path that has led to our present day understanding of the cluster responsible for water oxidation, this Article can provide little more than the briefest summary of this endeavor. Interested readers are directed to a series of excellent

(50) (a) Lundberg, M.; Siegbahn, P. E. M. *Phys. Chem. Chem. Phys.* **2004**, *6*, 4772. (b) Siegbahn, P. E. M.; Blomberg, M. R. A. *Philos. Trans. R. Soc. London, Ser. A* **2005**, *363*, 847. (c) Lundberg, M.; Blomberg, M. R. A.; Siegbahn, P. E. M. *Inorg. Chem.* **2004**, *43*, 264. (d) Lundberg, M.; Siegbahn, P. E. M. *Phys. Chem. Chem. Phys.* **2004**, *6*, 4772. (e) Siegbahn, P.; Crabtree, R. H. *J. Am. Chem. Soc.* **1999**, *121*, 117.

(51) (a) Spoviero, E. M.; Gascon, J. A.; McEvoy, J. P.; Brudvig, G. W.; Batista, V. S. *J. Chem. Theor. Comput.* **2006**, *2*, 1119. (b) Batista, V. S. *Philos. Trans. R. Soc. London, Ser. B*,in press..

(52) (a) Messinger, J.; Nugent, J. H. A.; Evans, M. C. W. *Biochemistry* **1997**, *36*, 11055. (b) Ahrling, K. A.; Peterson, S.; Styring, S. *Biochemistry* **1997**, *36*, 13148. (c) Messinger, J.; Robblee, J.; Yu, W. O.; Sauer, K.; Yachandra, V. K.; Klein, M. P. *J. Am. Chem. Soc.* **1997**, *119*, 11349.

(53) Yachandra, V. K.; Guiles, R. D.; McDermott, A.; Britt, R. D.; Cole, J.; Dexheimer, S. L.; Sauer, K.; Klein, M. P. *J. Phys., Colloq.* **1986**, *2*, 1121.

(54) Chan, M. K.; Armstrong, W. H. *J. Am. Chem. Soc.* **1990**, *112*, 4985.

(55) Afrati, T.; Dendrinou-Samara, C.; Raptopoulou, C. P.; Terzis, A.; Tangoulis, V.; Kessissoglou, D. P. *Angew. Chem., Int. Ed.* **2002**, *41*, 2148.

(56) (a) Alexiou, M.; Dendrinou-Samara, C.; Karagianni, A.; Biswas, S.; Zaleski, C. M.; Kampf, J.; Yoder, D.; Penner-Hahn, J. E.; Pecoraro, V. L.; Kessissoglou, D. P. *Inorg. Chem.* **2003**, *42*, 2185. (b) Alexiou, M.; Zaleski, C. M.; Dendrinou-Samara, C.; Kampf, J.; Kessissoglou, D. P.; Pecoraro, V. L. *Z. Anorg. Allg. Chem.* **2003**, *629*, 2348. (c) Zaleski, C.; Weng, T.-C.; Dendrinou-Samara, C.; Alexiou, M.; Kanakaraki, P.; Hsieh, W.-Y.; Kampf, J. W.; Penner-Hahn, J. E.; Pecoraro, V. L.; Kessissoglou, D. P. submitted to *Inorg. Chem.*

(57) (a) Kessissoglou, D. P.; Kirk, M. L.; Lah, M. S.; Li, X.; Raptopoulou, C.; Hatfield, W. E.; Pecoraro, V. L. *Inorg. Chem.* **1992**, *31*, 5424. (b) Kessissoglou, D. P.; Kirk, M. L.; Bender, C. A.; Lah, M. S.; Pecoraro, V. L. *J. Chem. Soc., Chem. Commun.* **1989**, 84. (c) Li, X.; Kessissoglou, D. P.; Kirk, M. L.; Bender, C. A.; Pecoraro, V. L. *Inorg. Chem.* **1988**, *27*, 1.

(58) (a) Kulik, L. V.; Epel, B.; Lubitz, W.; Messinger, J. *J. Am. Chem. Soc.* **2007**, *129*, 13421. (b) Kulik, L. V.; Epel, B.; Lubitz, W.; Messinger, J. *J. Am. Chem. Soc.* **2005**, *127*, 2392.

reviews that describe the shifting thoughts from manganese cubane-like clusters,[59] to independent trimer plus monomers,[57,60] to dimer of dimers,[61] and ultimately to the dangler model[30] (or a general tetranuclear 3 + 1 model[44]). We also will not have time to discuss the past controversy on the location of Ca^{II} with respect to the manganese centers. Instead, we will begin with the thinking in the late 20th century where the controversy focused on the likelihood of a dimer of dimers topology versus a less symmetric 3 + 1 or dangler model and then move into the new millennium studies that have been dominated by crystallographic analysis of the system.

Earlier, we discussed the importance of XAS (using XANES) to establish the oxidation states of the manganese in the OEC. An even greater contribution of this technique has been the elucidation of the structure of the manganese center using extended X-ray absorption fine structure (EXAFS) spectroscopy, which provides element-specific metrical and coordination number/type information. It has been known for many years[62] that some of the manganese ions are linked at a 2.7 Å distance while either a Mn−Mn or Mn−Ca vector at 3.3 Å also existed.[62b] The 2.7 Å distance is the hallmark of manganese bridged with μ_2- or μ_3-oxo ligands as seen in numerous dimeric and higher nuclearity systems.[63] From these studies and knowledge of the EPR spectral behavior of the cluster, a variety of structural possibilities were proposed, with the structure that emerged as most interesting being the dimer of dimers. If one examines the literature of the 1990s, it is difficult to find a water oxidation model that does not invoke, at least in part, this topology. However, we[44,45,64] and others[65] were concerned about certain observations that seemed to be incompatible with such an orientation of the manganese ions. Chief among these issues for us was the observation of a second S_2 EPR signal[21] at low field ($\sim g = 4$) that could be formed under conditions alternative to those responsible for the $g = 2$ multiline signal described by Dismukes. It was shown using EXAFS that the manganese cluster that exhibited this low-field signal was essentially structurally invariant from that of the form giving the $g = 2$ multiline. Yet, the $g = 4$ signal had a ground state of higher spin multiplicity (probably $S = {}^5/_2$).[66] Given the oxidation assignments for S_2 ($Mn^{III}Mn^{IV}_3$) and the observation that all μ_2-oxo-bridged manganese complexes were antiferromagnetically coupled (even those protonated or alkylated),[67] it became clear that a simple dimer of dimers structure was unlikely, if not impossible. We realized that a more complex relationship between the manganese ions was necessary to explain the observed EPR features while also complying with the EXAFS constraints. It seemed necessary to us to have a more complex coupling scheme in order to achieve the higher spin ground state suggested by the S_2 low-field EPR signal. We proposed as an alternative the 3 + 1 structure shown in Figure 7A.[44]

At the same time that we were shifting our thinking to this 3 + 1 topology, Britt's group was completing a detailed analysis of the ESEEM spectra of the $g = 2$ multiline signal.[30] His group reasoned that the dimer of dimers model could not adequately explain this EPR signal and proposed that one must have a special manganese distinct from the other three manganese ions in order to reproduce properly the observed spectra. The topology originally proposed to account for this was a linear orientation of manganese ions, with a special fourth manganese that became known as "the dangler". It should be noted, however, that the arguments that Britt forwarded are perfectly consistent with the more three-dimensional model that we had proposed in Figure 7A.

At this point, there were two independent approaches that were casting doubt on the dimer of dimers model. Of course, any model derived from the sporting techniques of spectroscopy or magnetism are often a bit tenuous, and so it came as a great relief when the first X-ray structure of the OEC appeared to generally validate the idea that the manganese ions were arranged in a 3 + 1 configuration.[68] Unfortunately, there were issues with this structure including its low resolution and relatively poor modeling of the metal cluster. In addition, the workers could not address the issue of the presence or absence of calcium. A more satisfying model appeared a few years later, when Barber's group reported a slightly higher resolution diffraction set that could be refined with a new model to higher certainty.[69] More importantly, by varying the synchrotron energy, these workers were able to distinguish the location of the calcium atom with respect to the manganese atoms. Their model for the OEC is shown

(59) Brudvig, G. W.; Crabtree, R. H. *Proc. Natl. Acad. Sci. U.S.A.* **1986**, *83*, 4586. (b) DePaula, J.; Beck, W.; Brudvig, G. W. *J. Am. Chem. Soc.* **1986**, *108*, 4002.

(60) (a) Kessissoglou, D. P.; Butler, W. M.; Pecoraro, V. L. *J. Chem. Soc., Chem. Commun.* **1986**, 1253. (b) Kessissoglou, D. P.; Li, X. H.; Butler, W. M.; Pecoraro, V. L. *Inorg. Chem.* **1987**, *26*, 2487.

(61) Yachandra, V. K.; DeRose, V. J.; Latimer, M. J.; Mukerji, I.; Sauer, K; Klein, M. P. *Science* **1993**, *260*, 675.

(62) (a) Kirby, J. A.; Robertson, A. S.; Smith, J. P.; Thompson, A. C.; Cooper, S. R.; Klein, M. P. *J. Am. Chem. Soc.* **1981**, *103*, 5529. (b) DeRose, V. J.; Mukerji, I.; Latimer, M. J.; Yachandra, V. K.; Sauer, K.; Klein, M. P. *J. Am. Chem. Soc.* **1994**, *116*, 5239.

(63) (a) Cooper, S. R.; Dismukes, G. C.; Klein, M. P.; Calvin, M. *J. Am. Chem. Soc.* **1978**, *100*, 7248. (b) Larson, E.; Lah, M. S.; Li, X.; Bonadies, J. A.; Pecoraro, V. L. *Inorg. Chem.* **1992**, *31*, 373. (c) Larson, E.; Pecoraro, V. L. *J. Am. Chem. Soc.* **1991**, *113*, 3810. (d) Wang, S. Y.; Folting, K.; Streib, W. E.; Schmitt, E. A.; McCusker, J. K.; Hendrickson, D. N.; Christou, G. *Angew. Chem., Int. Ed.* **1991**, *30*, 305–306. (e) Bashkin, J. S.; Chang, H. R.; Streib, W. E.; Huffman, J. C.; Hendrickson, D. N.; Christou, G. *J. Am. Chem. Soc.* **1987**, *109*, 6502–6504. (f) Hendrickson, D. N.; Christou, G.; Schmitt, E. A.; Libby, E.; Bashkin, J. S.; Wang, S. Y.; Tsai, H. L.; Vincent, J. B.; Boyd, P. D. W.; Huffman, J. C.; Folting, K.; Li, Q. Y.; Streib, W. E. *J. Am. Chem. Soc.* **1992**, *114*, 2455.

(64) Law, N. A.; Kampf, J. W.; Pecoraro, V. L. *Inorg. Chim. Acta* **2000**, *297*, 252.

(65) Kirk, M. L.; Chan, M. K.; Armstrong, W. H.; Solomon, E. I. *J. Am. Chem. Soc.* **1992**, *114*, 10432.

(66) (a) Haddy, A.; Dunham, Wr.; Sands, R. H.; Aasa, R. *Acta Biochim. Biophys.* **1992**, *1099*, 25. (b) Horner, O.; Riviere, E.; Blondin, G.; Un, S.; Rutherford, A. W.; Girerd, J.-J.; Boussac, A. *J. Am. Chem. Soc.* **1998**, *120*, 7924.

(67) (a) Baldwin, M. J.; Gelasco, A.; Pecoraro, V. L. *Photosynth. Res.* **1993**, *38*, 303. (b) Baldwin, M. J.; Stemmler, T.; Riggs-Gelasco, P. J.; Kirk, M. J.; Penner-Hahn, J. E.; Pecoraro, V. L. *J. Am. Chem. Soc.* **1994**, *116*, 11349. (c) Baldwin, M. P.; Law, N. A.; Stemmler, T. L.; Kampf, J. W.; Penner-Hahn, J. E.; Pecoraro, V. L. *Inorg. Chem.* **1999**, *38*, 4801–4809. (d) Larson, E. L.; Riggs, P.; Penner-Hahn, J. E.; Pecoraro, V. L. *J. Chem. Soc., Chem. Commun.* **1992**, 102.

(68) Zouni, A.; Witt, H.-T.; Kern, J.; Fromme, P.; Krauss, N.; Saenger, W.; Orth, P. *Nature* **2001**, *409*, 739.

(69) Ferreira, K. N.; Iverson, T. M.; Maghlaoui, K.; Barber, J.; Iwata, S. *Science* **2004**, *303*, 1831.

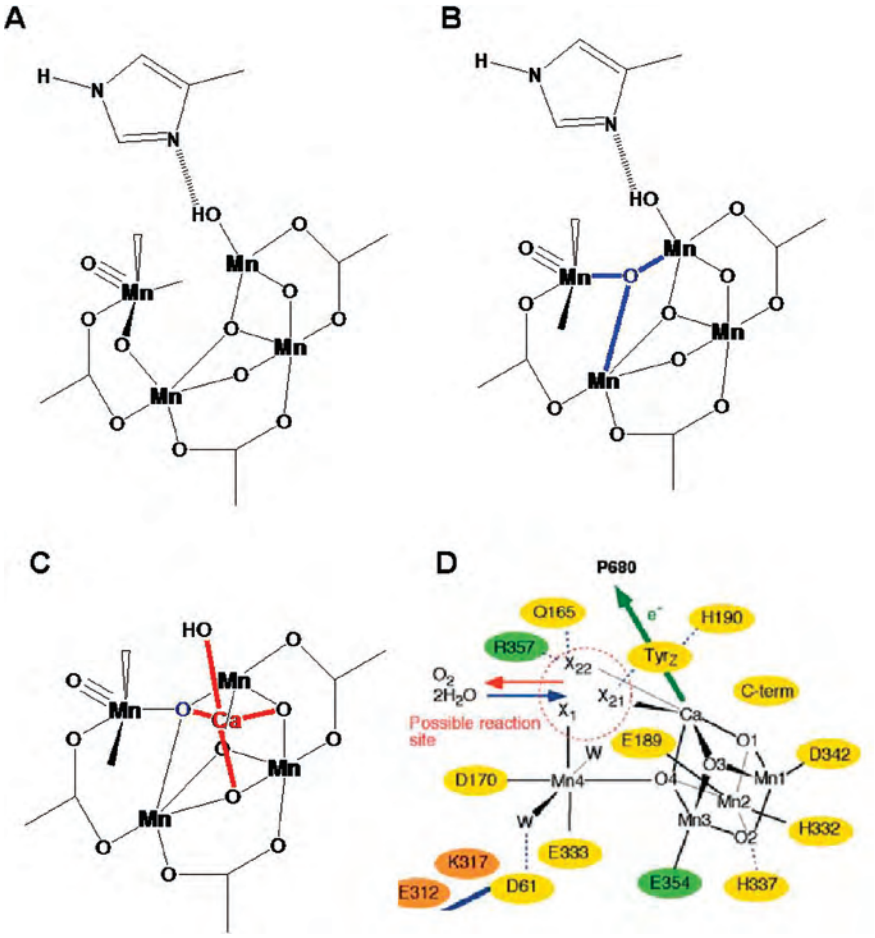

Figure 7. (A) Proposed structure of the Mn_4 cluster based on a magnetic analysis of the OEC in ref 44. (B) ChemDraw representation of the manganese ions as deduced from the Barber structure for the OEC. Notice that one bond has been broken and one added between manganese ions as compared to that given in part A. (C) The calcium ion has now been added to the Barber representation (D).

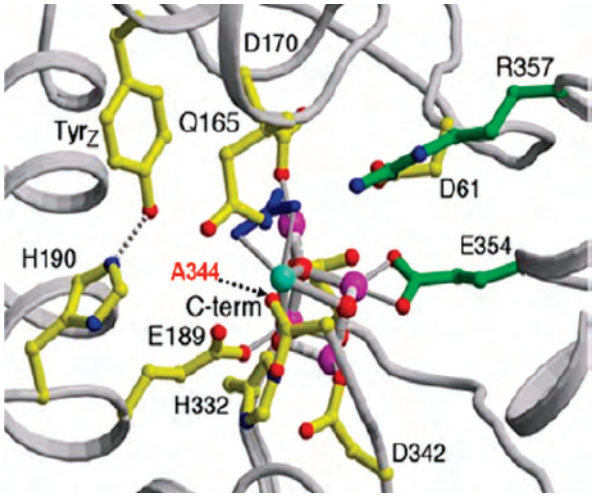

Figure 8. Mn_4Ca cluster derived from the Barber X-ray structure of the OEC. Reproduced with permission from ref 69.

schematically in parts B and C of Figure 7, and electron densities are given in Figure 8.

The Barber model places three manganese ions and one calcium ion in an $CaMn_3$ cubane-like cluster. The fourth manganese ion appears to be off to the side, "dangling" from the cluster as predicted by Britt and co-workers. As already stated, the original dangler model was presented as a linear topology so the general metal atom arrangement would not be expected to match the X-ray structure; however, if one considers the related 3 + 1 structure[44] shown in Figure 7, a direct comparison can be made. Remarkably, one needs to break only one bond and remake a new bond from the drawing shown as Figure 7A to obtain Barber's topology shown in Figure 7B. Thus, the structure predicted based on the sporting methods was in remarkably good accord with these crystallographic results. Of course, Ca^{II}, being diamagnetic, does not contribute directly to the magnetics and so could not be accounted for in the Figure 7A model. Its location is shown in Figure 7C, and one realizes immediately the impressive similarity between the X-ray structure and our prediction.

At times, it seems as if nothing in photosynthetic research stands the test of time and so it is, in part, with the crystallographic analysis. Yachandra et al. carried out a detailed study of the X-ray damage associated with the data collection on the X-ray crystals.[70] It had been assumed, though not really stated, that the structures that were appearing were of the S_1 state because it is the most stable form of the enzyme. However, it was shown that, under the high-intensity radiation necessary to collect diffraction data,

(70) Yano, J.; Kern, J.; Irrgang, K. D.; Latimer, M. J.; Bergmann, U.; Glatzel, P.; Pushkar, Y.; Biesiadka, J.; Loll, B.; Sauer, K.; Messinger, J.; Zouni, A.; Yachandra, V. K. *Proc. Natl. Acad. Sci. U.S.A.* **2005**, *102*, 12047.

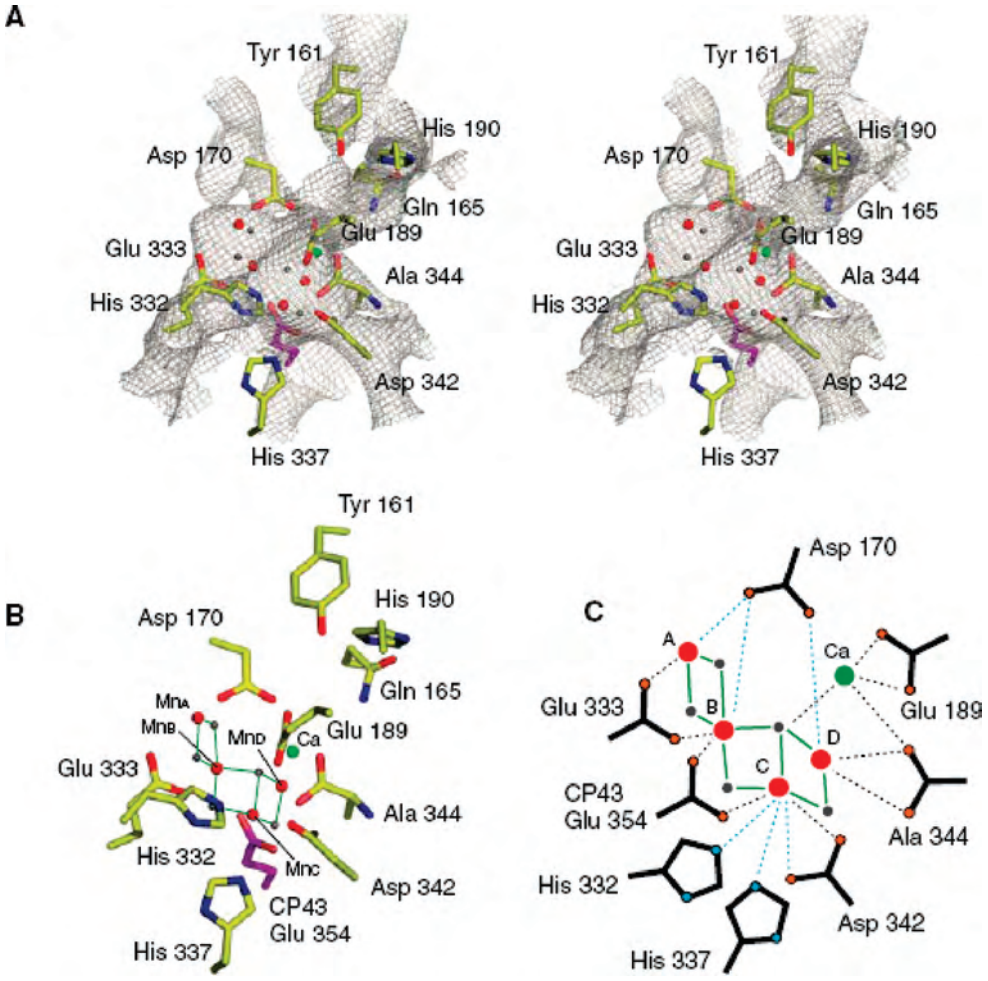

Figure 9. Multiple representations of the Mn_4Ca cluster based on polarized EXAFS data. Notice the shift in the position of the calcium ion with respect to the three manganese ions of the triangle. Also note in this model that a di-μ_2-oxo link to the dangler is suggested, which would restrict the Mn−Mn separation to a shorter distance. Reproduced with permission from ref 71.

there was rapid reduction of the manganese cluster. This observation, of course, throws into question the conclusions regarding the specific ligation and distance details from the crystallographic experiments. Certainly, one would expect some changes, possibly very large, upon reduction of an $Mn^{III}_2Mn^{IV}_2$ cluster to nearly all Mn^{II}. Fortunately, EXAFS experiments use a lower photon flux than is necessary for X-ray diffraction experiments so that data from this technique can still be used to assess structure. Furthermore, preparations of PS II that have been aligned can be used in oriented EXAFS experiments to propose a polarized EXAFS-derived model for the OEC.[71] This structure is given in Figure 9. Ironically, these authors have used the coordinates based on the X-ray structures to help orient the cluster, and a newer, higher-resolution structure has appeared from the Berlin group.[72] Our reading of this work is that while there are some important refinements to the structure proposed by Barber and movement of manganese/calcium atoms, the basic topology really is not altered dramatically (the Mn_3Ca structure no longer is a cubane being somewhat more distorted). Of course, what is significant to one person[71] is not to another, and so one may read an opposing view of this statement in a separate contribution in this issue. It should be noted, however, that the diagram in Figure 7A can as easily be converted into this EXAFS-derived topology as the structure proposed by Barber had been.

In summary, the most recent evidence strongly suggests that the manganese ions are arranged in a Mn_4Ca cluster. The structure is probably something like a Mn_3Ca cubane (or a distorted structure), with a fourth manganese atom linked to this cluster forming the dangler manganese that was predicted from spectroscopic and magnetic measurements. In the following section, we will now try to bring together all of the separate parts so far discussed (energetics, oxidation states, and structure) to assemble a model for the reactivity of the OEC and show how synthetic models are being used to test some of these ideas.

Model for Photosynthetic Water Oxidation

Instructors in general chemistry often refer to the number of grains of sand found on the beaches of the world in order to help students grasp the concept of a mole. An alternative

(71) Yano, J.; Kern, J.; Sauer, K.; Latimer, M. J.; Pushkar, Y.; Biesiadka, J.; Loll, B.; Saenger, W.; Messinger, J.; Zouni, A.; Yachandra, V. K. *Science* **2006**, *314*, 821.
(72) Loll, B.; Kern, J.; Saenger, W.; Zouni, A.; Biesiadka, J. *Nature* **2005**, *438*, 1040.

example could be the number of chemical models that have been proposed for photosynthetic water oxidation. For obvious reasons, we will not discuss all of these proposals, some of which appear in the complementary Articles of this issue. Instead, we will focus on a suggestion that appeared[45] in 1998 and that has been expanded on very thoughtfully by Brudvig and co-workers.[46]

For a number of years, we were focused on methods of generating dioxygen from a dimer of dimers model. Most promising in this regard were two observations for the reactivity of $[Mn(Salpn)(\mu_2\text{-}O)]_2$. The first of these was reported[73] by Boucher and Coe in which the acidification of this complex was reported to generate H_2O_2 and two Mn^{III}(Salpn)(solvent) molecules. The second report[74] came from our group in which we demonstrated that hydrogen peroxide underwent a vigorous catalytic reaction that generated dioxygen and regenerated the original manganese catalyst. Combining these two reactions led to a hypothetical system that would make dioxygen from water. Because of the importance of these observations, we explored more fully the hydrogen peroxide step. First, we demonstrated that the oxo groups of the complex could be protonated,[67] that this led to measurable changes in the structure and magnetics of the complex, and that these protons inhibit the catalase reactivity. More importantly, Law demonstrated in his Ph.D. thesis[75] that hydrogen peroxide was not formed by the addition of two proton equivalents to $[Mn(Salpn)(\mu_2\text{-}O)]_2$ but rather that the Salpn ligand was oxidized in the process. This discouraging observation occurred contemporaneously with our revised view of the manganese cluster as a 3 + 1 structure described above.

At this point, we realized that one of the manganese ions appeared to be structurally "special". Furthermore, the Berkeley group was acquiring strong evidence that the calcium atom was in close proximity to the manganese cluster. These two thoughts led us to propose a function for calcium that placed it in the heart of the water oxidation reaction, as shown in Figure 10. The idea sprang from the recognition that metalloenzymes containing alkali or alkaline-earth ions sometimes used these ions to polarize water molecules in order to facilitate a nucleophilic attack on a substrate. We reasoned that the special manganese may be able to reach the Mn^V oxidation level, which in the presence of water would likely be found as a $Mn^V{=}O$ moiety. This highly polarized oxo group should be particularly electrophilic and could, in principle, be attacked by a strongly nucleophilic hydroxide ion bound to Ca^{II}. The result would be a manganese(III) hydroperoxo species [Mn^{III}OOH], which could subsequently decompose with the redox assistance of the remaining trinuclear manganese assembly to S_0 and dioxygen. Brudvig and co-workers have nicely developed a detailed mechanism accounting for proton movement and oxidation through the *S* clock based on these ideas.[46]

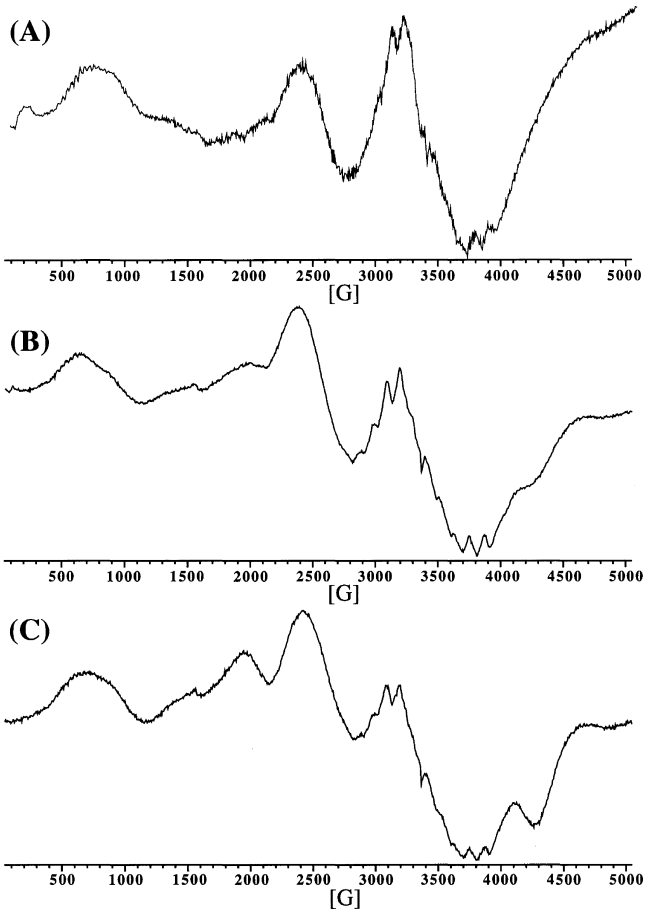

Figure 10. Perpendicular-mode EPR spectra of $\{Mn^{IV}{}_2(2\text{-}OHSalpn)_2OH\}^+$ at (A) 4.2 K, (B) 10 K, and (C) 16 K. The manganese complex was dissolved in butyronitrile (2 mM): microwave frequency, 9.432 GHz; power, 20 mW; modulation amplitude, 10 G; modulation frequency, 100 kHz.

The next issue for us as coordination chemists is to prepare molecules that can test aspects of this proposal. Several reports[76–78] have made claims for water oxidation using manganese model compounds. In these cases, high-valent manganese has been invoked in the critical oxidation step. While exciting, clearly more work is needed in this area, especially given controversies associated with the chemistry.[79]

Our efforts have focused on preparing manganese compounds for binuclear $Mn^{IV}Mn^V$ systems, particularly those containing the $Mn^V{=}O$ moiety. We have examined extensively the chemistry of ring-substituted derivatives of 2-OHSalpn with manganese.[80] Early in this Article,[13] we discussed the ability of this compound to be oxidized through multiple oxidation levels beginning with the Mn^{II} dimer $[Mn(2\text{-}OHSalpn)]_2{}^{2-}$ and progressing as high as the Mn^{III}/Mn^{IV} complex, $[Mn(2\text{-}OHSalpn)]_2{}^+$. The substitution of water leads to the asymmetric complexes $\{[Mn^{III}(2\text{-}OHSalpn)]_2H_2O\}$, $\{Mn^{III}Mn^{IV}$(2-

(73) Boucher, L. J.; Coe, C. G. *Inorg. Chem.* **1976**, *15*, 1334.
(74) Larson, E.; Pecoraro, V. L. *J. Am. Chem. Soc.* **1991**, *113*, 7809.
(75) Law, N. Models for the Reactivity of Mn di-μ2-oxo cores in the Oxygen Evolving Complex. Ph.D. Dissertation, University Microfilm, 1999.
(76) (a) Limburg, J.; Vrettos, J. S.; Liable-Sands, L. M.; Rheingold, A. L.; Crabtree, R. H.; Brudvig, G. W. *Science* **1999**, *283*, 1524. (b) Chen, H. Y.; Faller, J. W.; Crabtree, R. H.; Brudvig, G. W. *J. Am. Chem. Soc.* **2004**, *126*, 7345. (c) Limburg, J.; Vrettos, J. S.; Chen, H. Y.; dePaula, J. C.; Crabtree, R. H.; Brudvig, G. W. *J. Am. Chem. Soc.* **2001**, *123*, 423.
(77) Yagi, M.; Narita, K. *J. Am. Chem. Soc.* **2004**, *126*, 8084.
(78) Poulsen, A. K.; Rompel, A.; MacKenzie, C. J. *Angew. Chem., Int. Ed.* **2005**, *44*, 6916.
(79) Baffert, C.; Romain, S.; Richardot, A.; LePetre, J. C.; Lefebvre, B.; Deronzier, A.; Collomb, M.-N. *J. Am. Chem. Soc.* **2005**, *127*, 13694.
(80) Gelasco, A.; Pecoraro, V. L. *J. Am. Chem. Soc.* **1993**, *115*, 7928.

$OHSalpn)_2H_2O\}^+$, and $\{Mn^{III}Mn^{IV}(2\text{-}OHSalpn)_2OH\}$. We had independently shown[81] that the homolytic bond dissociation energies associated with the complexes were approximately 90 kcal/mol, suggesting that if we could make our solutions sufficiently basic, we should be able to prepare $\{Mn^{IV}{}_2(2\text{-}OHSalpn)_2OH\}^+$ from $\{Mn^{III}Mn^{IV}(2\text{-}OHSalpn)_2H_2O\}^+$ directly by electrochemical methods. Furthermore, we hoped that by using a proton-coupled electron-transfer process we would be able to access the desired $Mn^V{=}O$ species $\{Mn^{IV}Mn^V{=}O(2\text{-}OHSalpn)_2\}^+$ as well.

The second cyclic voltammogram in Figure 3 illustrates that the preparation of $\{Mn^{IV}{}_2(2\text{-}OHSalpn)_2OH\}^+$ from $\{Mn^{III}Mn^{IV}(2\text{-}OHSalpn)_2H_2O\}^+$ is readily achieved and we have isolated a solid that yields the desired physical properties for this species. The perpendicular-mode EPR spectra for this complex are shown in Figure 10. To our knowledge, this was the first reported example of a parallel-mode EPR spectrum of a Mn^{IV} dimer. Like the previously reported $[Mn^{IV}(2\text{-}OHSalpn)]_2{}^{2+}$, this complex also exhibits a perpendicular-mode EPR spectrum because of its weak antiferromagnetic exchange coupling. XANES spectra also confirm the assignment of the complex as Mn^{IV} because the edge energy for the resultant solid is 1.5 eV higher than that of the starting $\{Mn^{III}Mn^{IV}(2\text{-}OHSalpn)_2OH\}$, a difference consistent with numerous other $Mn^{III}Mn^{IV}$ to $Mn^{IV}{}_2$ oxidations.

Subsequent efforts to prepare the desired $\{Mn^{IV}Mn^V{=}O(2\text{-}OHSalpn)_2\}^+$ using an electrochemical approach were unsuccessful. We believe this to be true for two reasons. First, the $\{Mn^{IV}{}_2(2\text{-}OHSalpn)_2OH\}^+$ is not sufficiently basic to generate the necessary $\{Mn^{IV}{}_2(2\text{-}OHSalpn)_2O\}^{2+}$ precursor under standard conditions to carry out the metal oxidation. Under more basic conditions, $\{Mn^{IV}{}_2(2\text{-}OHSalpn)_2OH\}^+$ converts rapidly to the tetrameric $\{[Mn^{IV}{}_2(2\text{-}OHSalpn)_2]_2O\}^{2+}$ whose EPR spectrum was shown in Figure 6. We next explored alternative strategies for the preparation of the $Mn^{IV}Mn^V{=}O$ species.

It is well established that the reaction of certain oxo-transfer agents such as *m*-chloroperbenzoic acid (*m*-CPBA) or hypochlorous acid under basic conditions with Mn^{III}(Salpn) or Mn^{III}(Salen) causes olefin oxidation to the desired epoxide.[82,83] A quick comparison of Mn^{III}Salen and $\{Mn^{III}Mn^{IV}(2\text{-}OH\ Salpn)_2H_2O\}^+$ shown in Scheme 1 illustrates that the Mn^{III} ion has a similar coordination environment in both structures. We reasoned that $\{Mn^{III}Mn^{IV}(2\text{-}OHSalpn)_2H_2O\}^+$ should be capable of olefin epoxidation, as observed for Mn^{III}(Salen). Furthermore, though controversial,[84–88] it has been suggested that the active

Scheme 1

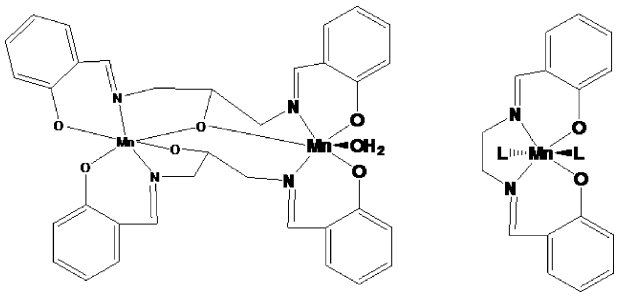

species of the Salen-based epoxidation reactions is a $Mn^V{=}O$ species. If true, then we should be able to chemically oxidize $\{Mn^{III}Mn^{IV}(2\text{-}OHSalpn)_2H_2O\}^+$ by two electrons using an oxo-transfer agent such as *m*-CPBA.

We tested whether the first portion of this proposition is true, that is, that $\{Mn^{III}Mn^{IV}(2\text{-}OHSalpn)_2H_2O\}^+$ in the presence of *m*-CPBA *n*-morphiline oxide (NMO) is capable of epoxidizing olefins. $\{Mn^{III}Mn^{IV}(2\text{-}OHSalpn)_2H_2O\}^+$ was reacted with *m*-CPBA in the presence of cyclohexene and NMO at −78 °C. Cyclohexene oxide was detected by gas chromatography (GC)−mass spectrometry (MS), whereas no 2-cyclohexen-1-ol or 2-cyclohexen-1-one was detected. Cyclohexene oxide is the direct product of the epoxidation via a concerted two-electron oxo-transfer process. In contrast, 2-cyclohexen-1-ol and 2-cyclohexen-1-one are allylic oxidation products generated through radical processes such as those shown by Caudle et al. for related systems.[13] The reaction proceeded for 20 turnovers based on a manganese catalyst. This reactivity could be taken as circumstantial evidence supporting the transient existence of the desired $Mn^{IV}Mn^V{=}O$. However, a troubling side reaction was observed, the oxidation of *m*-chlorobenzoic acid (mCBA) to *m*-chlorophenol. We investigated this chemistry with a known $Mn^V{=}O$ complex reported by Collins et al.[89] and also with Mn(Salen) and observed a rapid oxidation of the organic product, yielding the same *m*-chlorophenol product. While an X-ray structure of the Mn^VHMPAB complex[89] is known and we have shown using XANES spectroscopy that such a species is formed upon reaction of the Mn^{III} precursor with *m*-CPBA, the case of Mn(Salen) is more ambiguous.

Because of the rapid olefin epoxidation, we attempted to detect the $Mn^{IV}Mn^V{=}O$ species by adding 1 equiv of *m*-CPBA to $\{Mn^{III}Mn^{IV}(2\text{-}OHSalpn)_2H_2O\}^+$ in the absence of a substrate at −78 °C. The parallel-mode spectrum that results is identical with that observed in Figure 6. This is the same product formed by bulk oxidation in basic conditions, the tetrameric $\{[Mn(2\text{-}OHSalpn)]_4O\}^{2+}$. One explanation for this tetrameric product is that a comproportionation reaction between the starting $Mn^{III}Mn^{IV}$ dimer and the generated $Mn^{IV}Mn^V{=}O$ species occurs at near-stoichiometric oxidant concentration.

In an effort to surmount this difficulty, we next added a 500-fold excess of *m*-CPBA to the reaction solution. Gas evolution was immediately observed. In experiments that allowed us to trap and analyze the liberated head gas, we confirmed that CO_2

(81) Caudle, M. T.; Pecoraro, V. L. *J. Am. Chem. Soc.* **1997**, *119*, 3415.
(82) Zhang, W.; Loebach, J. L.; Wilson, S. R.; Jacobsen, E. N. *J. Am. Chem. Soc.* **1990**, *112*, 2801.
(83) Srinivasan, K.; Michaud, P.; Kochi, J. K. *J. Am. Chem. Soc.* **1986**, *108*, 2309.
(84) Campbell, K. A.; Lashley, M. R.; Wyatt, J. K.; Nantz, M. H.; Britt, R. D. *J. Am. Chem. Soc.* **2001**, *123*, 5710.
(85) Yin, G. C.; McCormick, J. M.; Buchalova, M.; Danby, A. M.; Rodgers, K.; Day, V. W.; Smith, K.; Perkins, C. M.; Kitko, D.; Carter, J. D.; Scheper, W. M.; Busch, D. H. *Inorg. Chem.* **2006**, *45*, 8052.
(86) Yin, G. C.; Buchalova, M.; Danby, A. M.; Perkins, C. M.; Kitko, D.; Carter, J. D.; Scheper, W. M.; Busch, D. H. *Inorg. Chem.* **2006**, *45*, 3467.
(87) Yin, G.; Danby, A. M.; Kitko, D.; Carter, J. D.; Scheper, W. M.; Busch, D. H. *J. Am. Chem. Soc.* **2007**, *129*, 1512.
(88) Yin, G.; Danby, A. M.; Kitko, D.; Carter, J. D.; Scheper, W. M.; Busch, D. H. *Inorg. Chem.* **2007**, *46*, 2173.
(89) (a) Collins, T. J.; Powell, R. D.; Slebodnick, C.; Uffelman, E. S. *J. Am. Chem. Soc.* **1990**, *112*, 899. (b) Collins, T. J.; Gordon-Wylie, S. W. *J. Am. Chem. Soc.* **1989**, *111*, 4511.

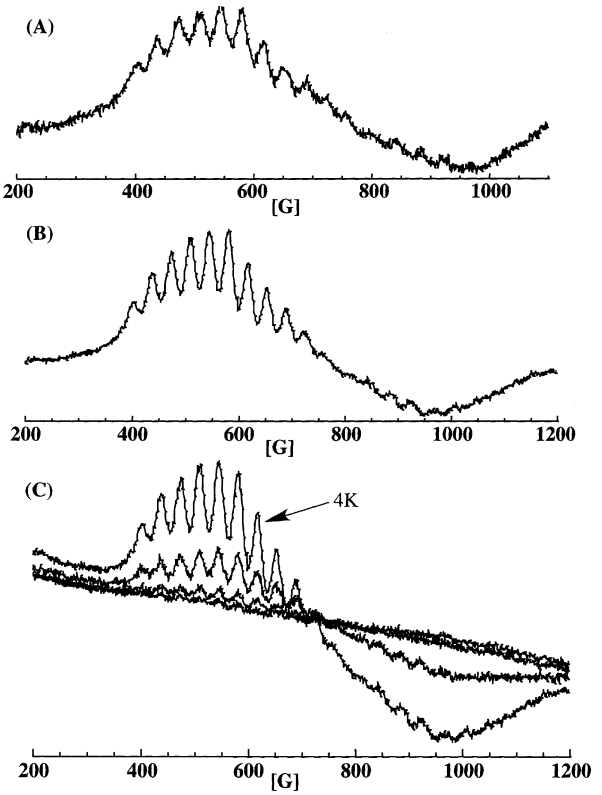

Figure 11. Parallel-mode EPR spectra of $\{Mn^{III}Mn^{IV}(2\text{-}OHSalpn)_2H_2O\}^+$ reacted with *m*-CPBA in acetonitrile at 20 °C. Freeze quench at various reaction times: (A) 30 ms; (B) 120 ms. (C) Temperature dependence from 4 K (top) to 40 K (bottom). EPR conditions for 4 K: microwave frequency, 9.424 GHz; power, 2 mW; modulation amplitude, 10 G; modulation frequency, 100 kHz.

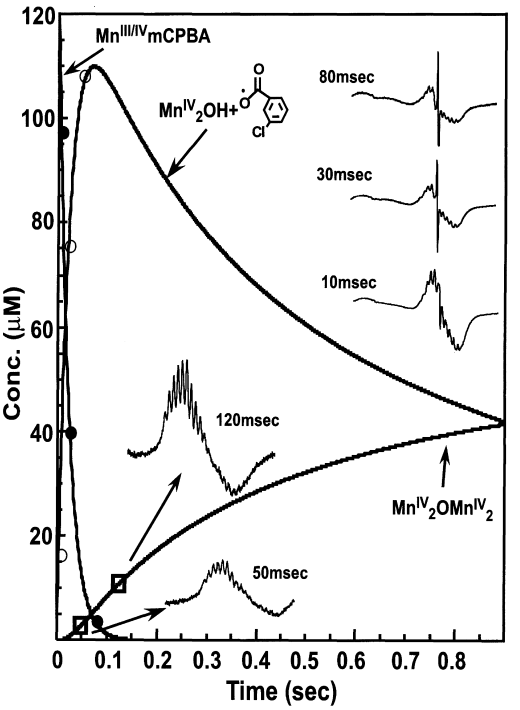

Figure 12. Species distribution plot from the stopped-flow data fitted to a biexponential model: A → B, 2B → 2C. Stopped-flow conditions: $[\{Mn^{III}Mn^{IV}(2\text{-}OHSalpn)_2H_2O\}^+] = 0.15$ mM; [*m*-CPB] = 4 mM, temperature = 5 °C, collection time = 1 s. Solid circles correspond to the concentration of $\{Mn^{III}Mn^{IV}(2\text{-}OHSalpn)_2H_2O\}^+$, open circles correspond to the concentration of $\{Mn^{IV}_2(2\text{-}OHSalpn)_2OH\}^+$, and open squares reflect the concentration of $\{[Mn(2\text{-}OHSalpn)]_4O\}^{2+}$. EPR spectra at designated time points are added to correlate the EPR behavior of samples as a function of time. EPR spectral conditions are given in Figure 11.

was being evolved. This observation is identical with that for the reaction of Mn(Salen) or Mn(HMPAB) with *m*-CPBA described above. Mass spectral analysis of the solution demonstrated that *m*-chlorophenol was also formed, indicating that the source of CO_2 was likely the *m*-CBA that was oxidized by the high-valent manganese complex. Under these conditions, the resultant EPR signal was that of the tetrameric compound, the growth of which is shown in Figure 11. Such a signal could be generated by the reaction of a $Mn^{IV}Mn^{V}$=O complex with *m*-CBA to generate the Mn^{IV} dimer and *m*-CBA radical. The radical would decompose to CO_2 plus the *m*-chlorophenyl radical, while the Mn^{IV} dimer would dimerize to give the observed tetramer. We have ruled out the possibility of a stable phenoxy radical as described by Wieghardt et al.[90] because the characteristic UV–vis bands for such radicals are not observed in this system.

Once again, all of these results are consistent with the formation of a $Mn^{IV}Mn^{V}$=O complex; however, there has been no direct spectroscopic detection of the species. Therefore, we carried out detailed stopped-flow kinetics and rapid freeze-quench EPR studies on the $\{Mn^{III}Mn^{IV}(2\text{-}OHSalpn)_2H_2O\}^+$/*m*-CPBA system to glean more insight on the early stages of this reaction. These data are summarized in Figure 12. Analysis of the stopped-flow data suggested that there were three primary species, which we will describe as A−C. During the first 100 ms, species A rapidly decays to near zero and species B rapidly rises to a maximum. The rapid freeze-quench perpendicular-mode EPR spectrum at 10 ms showed mostly the $g = 2$ signal that is characteristic of the starting $\{Mn^{III}Mn^{IV}(2\text{-}OHSalpn)_2H_2O\}^+$ and a very weak radical signal. Note that one would expect an $S = {}^3/_2$ signal for the $Mn^{IV}Mn^{V}$=O species because d^2 metal oxo species are invariably low spin. As the reaction time increases to 30 ms and then 80 ms, the radical signal intensifies while the $g = 2$ multiline weakens. At the same time in the low-field region, broad spectral features for $\{Mn^{IV}_2(2\text{-}OHSalpn)_2OH\}^+$ develop. We also observe a signal indicative of the tetramer developing from 50 to 120 ms. We conclude that the three EPR-observable manganese species are the starting $Mn^{III}Mn^{IV}$ dimer (species A), which converts into the Mn^{IV} dimer (species B) and the radical (*m*CBA radical), with species C being the ever-present tetramer. The simplest explanation from these experiments is that a $Mn^{IV}Mn^{V}$=O species could be formed in low concentration and with an extremely short half-life (<10 ms); however, we favor the proposal of Busch et al.[88] that the complexes both carry out their epoxidation chemistry and exist in the absence of a substrate as Mn^{IV} species, possibly with coordinated peroxides, not as Mn^{V}=O.

Summary

The experiments above demonstrate the extreme difficulty in clearly assessing chemical mechanism in many manganese redox reactions. All of the evidence is consistent with the

(90) Marlin, D. S.; Bill, E.; Weyhermuller, T.; Bothe, E.; Wieghardt, K. *J. Am. Chem. Soc.* **2005**, *127*, 6095.

formation of a $Mn^{IV}Mn^{V}$=O species; however, the definitive spectral evidence remains elusive. Such has been the behavior of PS II biophysics. One obtains evidence that is consistent with the ghost of the species desired, but always that intermediate (or maybe best transition state) is far too fleeting to actually capture. It is ironic that one must come to the same conclusion with the Salpn system that one draws from the photosystem, that either a highly reactive and undetectable Mn^{V}=O exists or some highly reactive and undetectable Mn^{IV} radical is the active agent. Future experiments will try to push back the time barriers in order to answer these important questions. Nonetheless, the progress in understanding the chemical aspects of water oxidation has progressed remarkably, on both the chemical and biological fronts, in the past 20 years, and one can only hope that similar major advances await us during the next 2 decades.

Experimental Section

Preparation of Complexes. $\{Mn^{III}Mn^{IV}(2\text{-OHSalpn})_2H_2O\}^+$ and $\{Mn^{III}Mn^{IV}(3,5\text{-di-}t\text{-Bu-2-OHSalpn})_2H_2O\}^+$ were prepared via literature procedures.[13] $\{Mn^{IV}{}_2(3,5\text{-di-}t\text{-Bu-2-OHSalpn})_2OH\}^+$ was prepared by the reaction of 0.53 g (0.4 mmol) [as a PF_6 salt] dissolved in 15 mL of dichloromethane/ether (1:1) with stirring. The solution was cooled to −40 °C in an acetonitrile/dry ice bath. Then $Ce^{IV}(t\text{-}Bu_4NH)_2(NO_3)_6$ (0.48 g, 0.482 mmol) was dissolved in 5 mL of cold dichloromethane, which was then added to the manganese solution at −40 °C. The solution was stirred for 10 min at −40 °C, and then it was suction-filtered at low temperature. The solvent was evaporated and dried at −25 °C under vacuum. The dark-brown solid was then redissolved in 15 mL of cold ether/pentane (2:1) at −50 °C. This solution was filtered and dried under vacuum, and the brown solid was collected and stored below −40 °C. $\{[Mn(2\text{-OHSalpn})]_4O\}^{2+}$ was prepared either by bulk oxidation of $\{Mn^{III}Mn^{IV}(2\text{-OHSalpn})_2H_2O\}^+$ in acetonitrile in the presence of a base or by the reaction of $\{Mn^{III}Mn^{IV}(2\text{-OHSalpn})_2H_2O\}^+$ with *m*-CPBA in acetonitrile at −15 °C.

Electrochemistry. Cyclic voltammograms for the complexes were measured under identical conditions using a platinum disk working electrode, an aqueous Ag/AgCl reference electrode, and a platinum wire counter electrode.

GC−MS. Cyclohexene, cyclohexene oxide, and NMO were purchased from Aldrich and used without further purification. *m*-CPBA was also purchased from Aldrich as a 50–60% pure sample and then was purified by dissolving the solid in dry methylene chloride, extracting with a saturated sodium bicarbonate solution several times, and then drying under vacuum for 1 day. The peroxy acid versus reduced acid ratio was determined by iodine titration to be 85%. The general methods for the epoxidation of organic substrates were that 1 equiv of manganese dimer was reacted with 100 equiv of cyclohexene and 100 equiv of NMO in dichloromethane. A total of 50 equiv of *m*-CPBA dissolved in dichloromethane was added to this solution at −78 °C. After 20 min, a portion of the mixture was collected and analyzed by GC−MS. A fixed amount of *n*-decane was added to each solution as an internal standard. The same reaction procedures were carried out at room temperature. Control reactions were carried out in the absence of a manganese complex. Authentic epoxide product and allylic oxidation products were used as standards. A Finnigan 4500 Quadrupole GC−MS spectrometer with an HP 5890 gas chromatograph equipped with a DB-5 capillary column installed in a splitless injector was used for these studies. The mass spectrometer is capable of unit mass resolution.

Stopped-Flow Experiments. The general sample preparations for the kinetic experiments were as follows: 12.8 mg of $\{Mn^{III}Mn^{IV}(2\text{-OHSalpn})_2\}PF_6$ was dissolved in 3 mL of 150 mM tetrabutylammonium perchlorate ($TBAClO_4$)/acetonitrile to make a 5 mM manganese stock solution. This stock solution was diluted with a 150 mM $TBAClO_4$ acetonitrile solution to make 0.1, 0.15, 0.2, 0.25, and 0.3 mM solutions. A total of 27 mg of *m*-CPBA dissolved in 5 mL of a 150 mM $TBAClO_4$/acetonitrile solution was then added to make a 20 mM stock solution. The stock solution was diluted with a 150 mM $TBAClO_4$/acetonitrile solution to make 0.1,0.5, 1.0, 2.0, and 4.0 mM solutions. These solutions were kept at 0 °C prior to reaction. The oxidation of $\{Mn^{III}Mn^{IV}(2\text{-OHSalpn})_2H_2O\}^+$ by *m*-CPBA was monitored using an Online Instrument System rapid scanning monochromator (OLIS-RSM) stopped-flow spectrophotometer equipped with a NESLab RTE 111 refrigerated bath/circulator. The reaction solutions were placed in two 2-mL syringes separately and submerged in a water bath maintained at 5 °C. The reactions were scanned at 1000 scans/s for 1 s. The reactions were monitored at 500 nm. Data were analyzed using the program *SPECFIT*.[91]

EPR Spectroscopy. X-band continuous-wave perpendicular-mode EPR spectra were collected either on a Bruker EMX200E spectrometer at the University of Michigan or a Bruker ESP300E spectrometer at Michigan State University. An Oxford Instruments ESR-900 continuous-flow crysostat was used to maintain a temperature between 4 and 60 K for both instruments. X-band continuous-wave parallel-mode detection experiments were collected at Michigan State University using the same experimental system as that described above. Experimental details for appropriate spectra are provided in the figure captions.

Rapid-Mix Freeze-Quench Spectroscopy. The freeze-quench experiments were performed at Michigan State University using an Update Instruments System 1000 Chemical/Freeze Quench apparatus (model 715 ram controller and model 1019 syringe ram). The manganese/*m*-CPBA solutions were placed in two equal-volume syringes and kept at room temperature. The syringe contents were combined in a Wiskind grid mixer (model 1155) at a ram velocity of 1.25 cm/s. Different reaction times were achieved by varying the length of the tubing (aging hose) connecting the mixer to the spray nozzle. The reaction mixture was ultimately sprayed from a 0.008-in.-diameter spray nozzle into a 4.5-in.-long fused quartz EPR tube equipped with a funnel filled with cold isopentane (HPLC grade, Sigma), which quenches the reaction in approximately 5 ms. The EPR tube and funnel were filled with isopentane and equilibrated for at least 5 min in a 8 L isopentane bath maintained at −140 °C with a LakeShore model 340 liquid-nitrogen bath. The frozen solids of an oxidized manganese solution were packed into the bottom of the EPR tube by using a precooled packing rod until a densely packed sample with a height of at least 1 cm was obtained. Time intervals for the quenching reaction of 10, 30, 80, 120, and 200 ms were employed.

Acknowledgment. V.L.P. acknowledges the NIH (Grant GM39406) for financial support of this work. We thank the EPR facility, especially Bryan Schmidt, at Michigan State University for access to and assistance with EPR and freeze-quench apparatuses.

IC7017488

(91) Stultz, L. K.; Binstead, R. A.; Reynolds, M. S.; Meyer, T. J. *J. Am. Chem. Soc.* **1995**, *117*, 2520.